TAO, Supplementary Issue, 165-182, March 1999

Direct Broadcast Experiment of Digital TV Signals on ROCSAT-1 ECP Payload

Yung -Chang Chen[1], Hsiao-Chuan Wang[1], Jean-Fu Kiang[2] and Mu-King Tsai[3]

(Manuscript received 6 November 1998, in final form 5 January 1999)

ABSTRACT

As one of the three communication experiments to be performed on the ECP payload of the LEO satellite ROCSAT-1, the direct broadcasting of digital TV signals using Ka-band experiment has been well planned and prepared. In this experiment, suitable compression and protection methods for the digitized video and audio signals in the LEO and Ka-band environments will be studied. The bitrate will be between 6.6 and 3.3 Mbps, depending on the affordable link budget. The carrier frequency of the uplink is 28.25 GHz, while that of the downlink is 18.45GHz. Because of the strong dependence of system performance on the channel characteristics, a realistic Ka-band channel model suitable for the subtropic Taiwan area will also be developed.

(Key words: Video and audio compression, Scalable coding, Ka-band characteristics)

1. INTRODUCTION

Due to progress in digital compression of TV signals, the direct-to-home (DTH) broadcasting services using satellites have become more and more popular. Direct broadcasting satellites (DBS) allow households to receive TV programs directly with small dishes. So far, C-band (4 ~8 GHz) and Ku-band (12~18 GHz) are widely used for DBS application, but they are becoming crowded. Ka-band (18~30 GHz) is preferred for next-generation wide-band multimedia communications, including direct TV broadcasting. Hence, the Republic of China, Taiwan has decided to carry out a series of Ka-band communication experiments, including the direct broadcasting experiment of digital TV signals.

ROCSAT-1 is a low-earth-orbit (LEO) satellite. The main advantage of using LEO satellites as compared to geosynchronous-earth-orbit (GEO) satellites is that the LEO satellites are closer to the earth, hence requiring less power. However, their orbit period around the earth is very short and the link time with any fixed ground receiver is on the order of a few minutes in each pass. A tracking antenna is needed at the ground station to track the satellite precisely.

[1]Department of EE, National Tsing-Hua University, Hsin-Chu, Taiwain, ROC
[2]Department of EE, National Chung-Hsing University, Taichung, Taiwain, ROC
[3]Department of EE, National Central University, Chung-Li, Taiwan, ROC

The link availability differs among different passes and is time-varying during a pass. The communication in the Ka-band generally suffers a high level of rain attenuation, in addition to some scintillation, and gaseous attenuation. The rain attenuation is stronger in the higher frequency bands, and significantly affects the communication quality [1]. All these factors should be taken into consideration for designing suitable compression and protection methods for the digitized video and audio signals.

In the experiment, video and audio signals are firstly compressed to 6.6/3.3 Mbps and their intermediate source bitrate. Added with suitable channel codes, the bit stream is then transmitted to the satellite and sent back to the ground station by the satellite transponder. The carrier frequency of the uplink is 28.25 GHz, while that of the downlink is 18.45 GHz.

For the compression of video signals, the Grand Alliance / MPEG2 standard [2], which becomes the ATSC ATV standard, is adapted, and two-layer coding schemes, not included in the standard, are designed. By using this scalable coding method, the video signal is adjusted with respect to changes of the link budget. Thus, the received video quality can be maintained when the satellite's transmission rate is reduced due to poor weather conditions. Under normal situations, the received quality should be better than, or at least the same as, that of a commercial VHS VCR.

For audio compression, the Dolby AC-3 format is applied to meet the specifications of ATSC ATV. Encoders and decoders are designed in this study. Also, encoding protection is studied in order to maintain good audio quality under strong noise interference.

In the system design, channel coding and Ka-band channel characteristics must be considered due to their impact on the video/audio signal transmission. In this work, we develop a channel simulation program for ROCSAT-1, into which the characteristics of rain attenuation in the Ka-band are incorporated. Realistic orbital parameters, power level, antenna radiation patterns, transmission data rate, and internal noise sources are chosen [3]. This channel simulation program is used to help design effective packet protection and a channel coding scheme which minimizes the deterioration to the received signals.

Figure 1 shows the block diagram of the proposed broadcast experiment system. The whole system was thoroughly simulated before the launch of ROCSAT-1. The simulation results will be compared with measurements when the satellite is launched. After the completion of experiments over two years, a realistic Ka-band channel model suitable for the subtropic Taiwan area will also be developed.

Section 2 sketches the entire system design, including the scalable video codecs design, and the feasibility study of unequal error protections.

Section 3 describes the format of a AC-3 bit stream and its error detection method. A simulation of BER on the AC-3 follows.

Section 4 discusses the attenuation mechanisms in the Ka-band, including three rain attenuation models and internal device noises. Then, the link budget calculation is presented to assess the carrier-to-noise ratio at the receiver, followed by the simulation scheme and results.

Section 5 gives concluding remarks.

2. BROADCAST SYSTEM DESIGN

The upper part of Figure 1 shows the procedures of the proposed encoder. The video

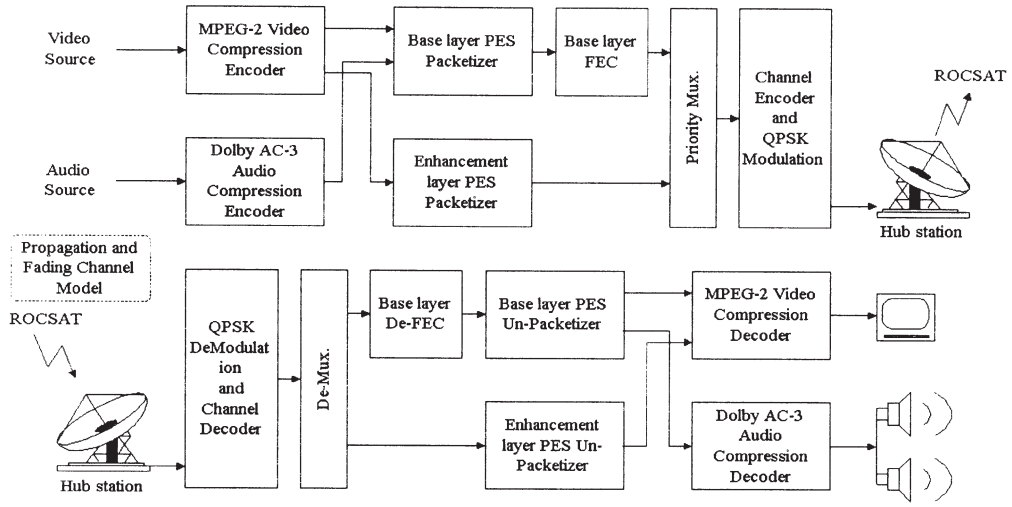

Fig.1. System block diagram of the direct TV broadcast experiment.

encoder compresses a sequence of source videos by MPEG-2 scalable coding and provides compressed bit streams with two priorities. One is the higher-priority base-layer video stream and the other is the second-layer video stream of lower priority. In the meantime, the audio encoder compresses the associated audio source and sends its output into the base-layer packetizer also. There, the audio bit stream and the base-layer video stream are packetized into packetized elementary streams (PES), respectively, and multiplexed together. The base-layer PES are then extra protected by the base-layer FEC, while the second-layer video stream is packetized into second-layer PES and sent directly to transport stream multiplexer without extra protection. After the process of built-in channel encoding with RS coder, interleaver and convolution coder, the bit stream is QPSK or BPSK modulated and transmitted into the Ka-band channel. The bottom part of Figure 1 shows the associated receiver that performs the inverse operations to the upper part.

2.1 Video Codecs Design

For the video coding system, backward compatibility to the current international standards is needed. To observe compatibility with the digital video broadcasting standards, our entire video coding system follows the MPEG-2 international standard.

Scalability is a tool standardized by MPEG-2 that supports applications beyond those addressed by the basic MAIN profile coding algorithm. The intention of scalable coding is to provide interoperability between different services and to flexibly support different functionalities of receivers. However, another important purpose of scalable coding is to provide a layered video bit stream with error resilience capability. The base layer is encoded to support a base quality of video, and is therefore regarded as critical information that needs to be correctly received by the decoder. An additional second-layer is transmitted with fewer

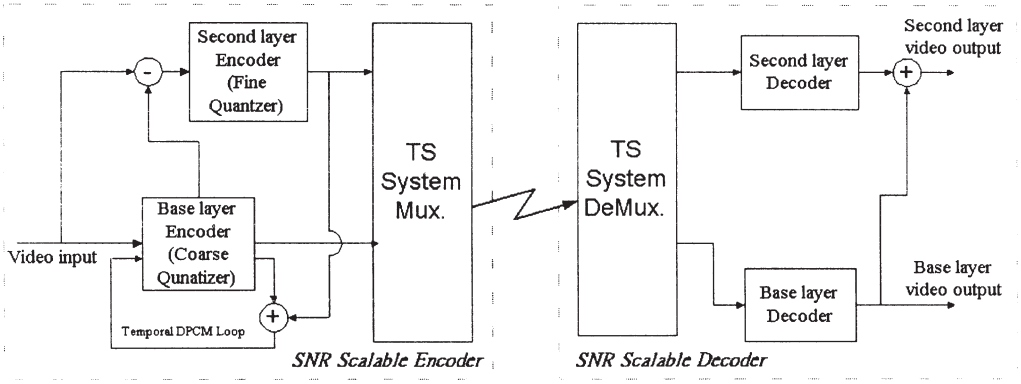

Fig. 2. Block diagram of SNR scalable encoder and its associated decoder.

protections. The scalability hence increases the link availability of a transmission channel. According to this outstanding property, we were motivated to study scalable codecs for the Ka-band ROCSAT-1 [4].

In MPEG-2, SNR scalability is a mechanism to provide two scales of SNR quality of decoded video through two encoded bit streams. Figure 2 depicts a general codec system of SNR scalability. The quantized DCT coefficients from the base layer (after being inverse-quantized) are subtracted from the output DCT blocks. The resulting quantization error is then requantized in the second layer by a finer quantizer. On the decoder side, the decoded DCT coefficients of both layers are added to obtain a high quality video. Otherwise, the base layer itself can be retrieved to show the base layer quality video. The design issue for SNR scalability is to develop the most effective encoding structure and its associated robust decoder, subject to the MPEG-2 specifications for the SNR scalable decoder [5].

Spatial scalability is applied where video needs to be decoded and displayed at multiple resolution scales. In MPEG-2, spatial scalability is to provide two scales of video resolution through two encoded bit streams. To design the spatial scalable encoder, we require two separate and loosely coupled MPEG-2 single layer encoders, as shown in Figure 3. Similar to SNR scalability, the design issues here are the effective encoding structure and robust decoder, subject to the MPEG-2 specifications for the spatial scalable decoder [4].

For scalable coding, prioritized transmission should be provided to enable the capability of error resilience. However, in satellite communication, the probability of errors is uniform for all of the transmitted information. A mechanism to support different degrees of protection on the bit streams of the scalable encoder is also required, subject to the built-in channel coding, described in the following section, and the channel characteristics. In [6], a base-layer FEC is proposed to provide unequal error protections.

2.2 Unequal Error Protections on Video Streams

Two methods can be used to provide different degrees of error protection on both layers during simultaneous transmission. The first one is to transmit the two layer bit streams by two

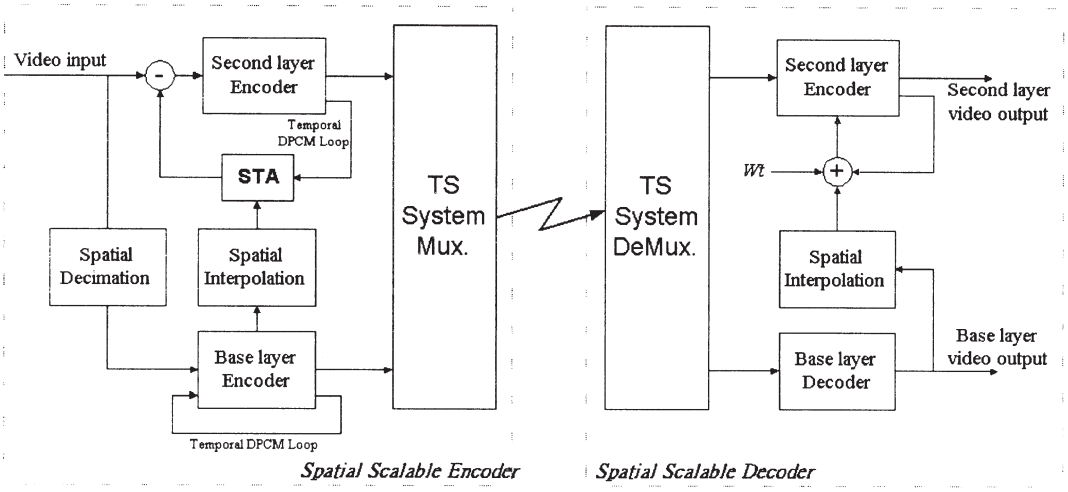

Fig. 3. Block diagram of the proposed spatial scalable codec model.

separate transponders. Different modulation schemes can be used to provide different degrees of error protection. For example, though binary phase-shift keying (BPSK) and quaternary phase-shift keying (QPSK) have the same equation on the average probability of bit errory

$$P_b = Q\left(\sqrt{2T_bB\frac{C}{N}}\right) \tag{1}$$

the bit duration-bandwidth product T_bB is different with the same carrier-to-noise ratio (C/N). For BPSK, T_bB=1 because one symbol represents one bit. For QPSK, T_bB = 0.5 because one symbol represent two bits. Therefore, under the same transmission power (power control is not practical in this high data rate and link-budget critical case.) and with different modulation schemes, different error probabilities can be obtained for both scalable layers. For instance, if the carrier -to- noise ratio C/N=4.7dB, the average probability of bit error in the QPSK system is 4.3×10^{-2}, while that in the BPSK can be 7.7×10^{-3}. Hence the base layer can be transmitted by using BPSK with fewer errors. Unfortunately this method will not be adopted in this broadcasting experiment because only one high speed transmitter and transponder can be used.

To reduce channel errors effectively, a typical channel coding system for broadcasting is a concatenated code. Two levels of coding, an inner code and an outer code, are concatenated to achieve the desired performance. The inner code, which interfaces directly with the modulator/demodulator and the channel, is usually configured to correct most of the channel errors. The outer code, usually a higher-rate and low-redundancy code, then further reduces the error probability to a specified level.

The most popular concatenated coding system uses a Viterbi-decoded convolutional inner code and a Reed-Solomon (RS) outer code, with an interleaver between the two coding stages. Because the output errors of the Viterbi-decoded system tend to be bursty, the follow-

ing RS outer code performs well in correcting a limited length of bursty errors. However, the concatenated system is severely degraded by correlated errors among successive symbols. Hence, the interleaver between the inner and outer codes needs to take place to randomly distribute the bursty errors into the neighboring blocks.

In the broadcasting experiment, this concatenated system is adopted as the built-in channel coding system. The RS outer code is (225, 205), which is a shortened version of the (255, 239) RS code. The maximum number of correctable erroneous bytes in a codeword is therefore 10. For the inner code, the considered convolutional code for experimental tests is $1/2$, $3/4$ and $7/8$. The interleaver depth is 4.

For unequal error protection, one method is to design a second FEC scheme in addition to the original channel coding. The algorithm is described in the following four steps :

Step 1: Segment the video elementary stream of the base layer into 181-byte packets sequentially.

Step 2: For each 181-byte packet, add a (201, 181) RS code as the second FEC.

Step 3: Segment the encoded bit stream of Step 2 into 201-byte packets. Note that the segmenting start point should be located at 100 bytes before the RS code of step 2. After the packet is obtained, add 4 bytes of TS header before the packet. The packet length therefore becomes 205 bytes.

Step 4: For each 205-byte packet from Step 3, perform the (225, 205) RS code provided in the built-in channel coding system.

Another method for unequal error protection is to bypass the built-in channel code system and design separate channel codes for each of the two layer streams. Optimal channel coding remains to be studied.

3. ERROR DETECTION METHOD FOR AC-3 BIT STREAM

3.1 Format of AC-3 Bit Stream

AC-3 is a digital audio compression algorithm for many digital audio systems. It is also a standard documented by the United States Advanced Television Systems Committee for HDTV transmission [7]. The AC-3 encoder can convert a 5.1 channel program from a PCM representation with 5.184 Mbps into a bit stream below 640 kbps. Such reduction of digital information for representing the audio signal benefits the satellite audio transmission, the terrestrial audio broadcasting, the delivery of audio over cables, and the audio storage in media.

An AC-3 bit stream is a sequence of synchronization frames. Each frame contains 6 coded audio blocks (AB). An audio block contains 256 audio samples. At the beginning of each frame, there is a synchronization information (SI) header which contains the information needed to acquire and maintain the synchronization. A CRC word (crc1) for covering the first 5/8 of the frame is also in the SI header. Following the SI header, there is a bit stream information (BSI) header that contains parameters describing the coded audio service. At the end of each frame is another CRC word (crc2) for covering the entire frame. Before the CRC word (crc2), there is an auxiliary data field (AUX). Both CRC words are 16-bit in length. Figure 4 shows the format of the AC-3 synchronization frame.

SI	BSI	AB0	AB1	AB2	AB3	AB4	AB5	AUX	CRC

Fig. 4. Format of AC-3 synchronization frame.

3.2 Error Detection in AC-3

At the receiving end, the AC-3 decoder checks the CRC words. A CRC check is reliable to 0.0015%. Usually, when an error is detected in the CRC check, the entire frame is discarded and the preceding frame is repeated to fill up this missing frame. When the transmission passes through an adverse environment, the quality of the decoded audio may be seriously degraded because too many frames are lost.

In order to know the effect of noise disturbance due to missing frames, we focus on a case of Mode 010 (2 channels, L and R) of AC-3. The audio source is samples played from a CD player. The two-channel audio is sampled in 16-bit PCM with a sampling rate of 44.1 kHz. Eight audio samples are used for testing; they are (1) flute, (2) symphony, (3) Japanese opera, (4) snare drum, (5) piano, (6) voice of female, (7) saxophone, and (8) voice of male. The encoded bit rate is set at 256, 192, 128, and 96 kbps. The difference between the original signal and the decoded signal in PCM is considered noise due to the audio compression mechanism. The signal-to-noise ratio (SNR) is calculated by the following equation,

$$\mathrm{SNR} = 10\log_{10}\frac{\sum_{\mathrm{i}}\chi^2(\mathrm{i})}{\sum_{\mathrm{i}}[\chi(\mathrm{i})-\hat{\chi}(\mathrm{i})]^2} \quad (\mathrm{dB}), \tag{2}$$

where $\chi(\mathrm{i})$ and $\hat{\chi}(\mathrm{i})$ are the original signal and the decoded signal, respectively. Table 1 shows the SNRs of the test audio samples.

SNR may not be an exact indicator of quality, but it is a good reference in our study. A subject listening test shows that the decoded audio has almost the same quality as the original for those cases with SNR higher than 18.

3.3 Simulation of BER on AC-3 Coding

In order to examine the effect of bit-error in the AC-3 bit stream, we artificially insert random patterns of bit-errors into the encoded bit stream. The bit-error-rate (BER) is set to be 0.0001%, 0.001%, 0.01%, and 0.1%, respectively. In fact, we can roughly estimate the toleration of bit-error-rate for different encoded bit-rates by inverting the frame length. Table 2 gives a rough estimate. We can see that a 256 kbps bit stream is totally destroyed when the BER is higher then 0.01%. The simulated results for the case of 256 kbps coding are listed in Table 3. The sampling rate is 44.1 kHz.

It is observed that audio quality degrades drastically when the BER is higher than 0.001%. The test samples become almost totally intolerable when the BER is equal to 0.01%. This is consistent with the prediction in Table 2.

Table 1. SNRs (dB) of the test samples.

Test sample		Channel	Bit rate (kbps)			
			96	128	192	256
1	Flute	L	12.13	14.47	15.38	15.46
		R	11.57	15.25	17.22	17.40
2	Symphony	L	10.85	14.93	17.96	18.41
		R	9.97	15.28	20.54	21.61
3	Japanese opera	L	7.30	7.76	7.91	7.94
		R	7.79	8.40	8.66	8.70
4	Snare drum	L	9.67	10.10	10.26	10.28
		R	10.56	11.43	11.74	11.76
5	Piano	L	14.25	18.54	20.18	20.28
		R	13.71	20.63	25.99	26.49
6	Voice of female	L	12.74	14.97	15.74	15.81
		R	11.90	17.33	23.12	23.95
7	Saxophone	L	10.28	10.40	10.41	10.42
		R	16.27	18.11	18.43	18.45
8	Voice of male	L	9.18	12.60	14.38	14.50
		R	7.85	8.29	8.39	8.40

3.4. Error Detection in Audio Blocks

The error detection in AC-3 is based on two CRC words in a frame. Any CRC check fail results in losing the entire frame. Several error correcting methods can be applied to restore the bit-stream. Usually, the price is to increase the bit rate and the computation time. For example, BCH(15,11,3) requires 15 bits to encode 11-bit information. Its capability is to correct one bit error in an 11-bit stream, but requires 36% more in bit count. This approach is unrealistic if we want to protect the entire synchronization frame. Our proposed method is to check audio blocks instead of the entire frame so that we may discard one of six audio blocks instead of the entire frame when an error appears in an audio block. This approach relies on information about location and the length of each audio block. This information depends on decoding the con-

Table 2. Toleration of bit-error-rates.

Nominal bit rate (kbps)	Frame length (bits)	Toleration of BER
256	8928	0.000112
192	6688	0.000149
128	4464	0.000224
96	3344	0.000299

* Sampling rate = 44.1 kHz

Table 3. SNRs (dB) of the test samples distorted by different BERs.

Test sample		Channel	Bit error rate				
			no	0.0001%	0.001%	0.01%	0.1%
1	Flute	L	15.46	15.14	11.67	4.03	0
		R	17.40	16.86	12.24	3.93	0
2	Symphony	L	18.41	17.84	12.31	1.89	0
		R	21.61	20.42	12.92	1.84	0
3	Japanese opera	L	7.94	7.88	6.94	1.47	0
		R	8.70	8.62	7.55	1.33	0
4	Snare drum	L	10.28	10.25	8.00	1.93	0
		R	11.76	11.71	9.44	3.22	0
5	Piano	L	20.28	19.75	12.72	1.79	0
		R	26.49	24.30	12.37	2.47	0
6	Voice of female	L	15.81	15.50	11.86	2.11	0
		R	23.95	22.15	13.84	1.35	0
7	Saxophone	L	10.42	10.26	8.96	2.04	0
		R	18.45	17.63	12.69	2.01	0
8	Voice of male	L	14.50	13.32	8.60	2.56	0
		R	8.40	8.27	6.86	2.17	0

*Encoded bit rate = 256 kbps

tents in BSI header and the parameters and exponents in the audio block. The contents in an audio block can be represented in three fields, as shown in Figure 5.

During the decoding process, the length of an audio block can be calculated according to its parameters and exponents. The length may be changed if its parameters or exponents have been disturbed. The proposed method is described as follows.

(1) In the encoder:

i) Calculate the length of each audio blocks. (in 11 bits).

ii) Use Hamming code to encode 11-bit block length into a pattern of 15 bits.

iii) Store the coded block lengths in the field "addbsi" of BSI.

(2) In the decoder:

Check crc1 and crc2. If no error appears in CRC checks, the frame is correct. Otherwise, we perform the following procedure;

i) Check for the availability of field "addbsi".

ii) Extract the block length of each audio block from "addbsi".

iii) Decode each audio block and calculate its length and location.

Fig. 5. Contents in an audio block..

iv) Discard the audio block if its length not can match the length specified in "addbsi".
v) Repeat the preceding audio block to fill up the missing block.

This method requires 90 more bits in the field "addsbi" of BSI. Where bit rate is equal to 256 kbps, as shown in Table 2, 90 bits are needed to specify the audio block lengths so that only 8838 bits are used for encoding the audio signal. This implies a slight quality degradation. Our experiment shows that the SNR is affected by less than 0.02 dB if there no bit errors appear in the bit-stream.

By our proposed method, if an audio block is missing, the preceding one is added in its place. However, when the error appears in BSI, all the following audio blocks become incorrect. This will cause the entire frame to be lost. Since the length of an audio block is about 1/6 of the entire frame, the tolerant of BER can be improved by around six times. A simulation like that in Table 3 has been conducted to demonstrate our proposed method. The results are shown in Table 4.

Comparing Table 3 and Table 4, we can see that SNRs have been increased for all the BER cases. Where BER is equal to 0.00001, the improvement is about 2~3 dB. Where BER is equal to 0.0001, the improvement is around 1.5 dB.

4. CHARACTERISTICS OF THE KA-BAND CHANNEL

Communication performance is determined mainly by the carrier-to-noise ratio at the receiver. The received power level mainly is determined by the transmitted power level, free space loss, transponder gain, antenna gains and various kinds of fadings. The noise power can be expressed in terms of the noise temperature, and is determined by rain attenuation, gaseous attenuation, internal loss, interferences and other loss mechanisms.

4.1 Rain Attenuation

Three rain models are considered in this work. They are the Crane model [8], the ITU-R model [9], and the DAH model [10]. The Crane and the ITU-R models have been widely used for global prediction. However, the newly developed DAH model is claimed to make better predictions than the other two models.

The Crane model is an empirical model based on the point rain rate distribution, vertical rain extent (height of 0°C isotherm), path length immersed in the rain, and frequency-dependent coefficients derived from raindrop characteristics [8]. The point rain rate can be looked up in tables categorized according to the rain climate region [11].

The ITU-R model predicts the attenuation based on effective rain height (function of the station latitude), path length through the rain cell, rain intensity at 0.01 percentile, wave polarization, and frequency-dependent coefficients which can be interpolated from a lookup table [9].

The DAH model is a modification of the ITU-R model, in which two adjustment factors are proposed to refine the predictions [10].

Among these three rain models, the ITU-R and the DAH models use the rain rate $R_{0.01}$ of

Table 4. SNRs (dB) of the test samples based on the proposed method.

Test sample		Channel	Bit error rate				
			no	0.0001%	0.001%	0.01%	0.1%
1	Flute	L	15.46	15.28	13.22	6.31	1.20
		R	17.40	17.19	14.27	5.30	1.03
2	Symphony	L	18.41	17.89	15.23	3.90	0.53
		R	21.61	20.53	16.44	4.05	0.55
3	Japanese opera	L	7.94	7.92	7.33	1.97	0.79
		R	8.70	8.67	7.99	2.22	0.73
4	Snare drum	L	10.28	10.26	9.77	2.83	0.78
		R	11.76	11.72	11.20	3.72	1.07
5	Piano	L	20.28	19.96	15.82	4.30	0.76
		R	26.49	25.18	17.71	5.53	0.79
6	Voice of female	L	15.81	15.63	13.62	3.80	0.82
		R	23.95	22.99	16.80	4.06	0.99
7	Saxophone	L	10.42	10.35	9.57	3.09	0.69
		R	18.45	17.96	14.61	3.57	0.75
8	Voice of male	L	14.50	14.18	12.12	3.56	0.80
		R	8.40	8.34	7.84	2.89	0.81

*Encoded bit rate = 256 kbps

an average year to estimate the attenuation at other rain rates, while the Crane model uses the expected rain rate to estimate the attenuation. The attenuation predicted by these three models for Tainan, Taiwan (23°N) is shown in Figure 6 where the Crane climate rain rate distribution is used. To obtain more reliable predictions, all three models are considered in our simulation, and the local rain rate distribution in Tainan is used instead of the Crane rain rate distribution.

In a clear sky, gaseous absorption is the main source of the link noise. It consists of oxygen absorption and water vapor absorption. Both can be estimated by using empirical formulas which are functions of frequency. At f = 30 GHz and at an elevation angle of 20°, the water vapor absorption is less than 1 dB even with a high water vapor density of 10 g/m^3. The oxygen absorption is in the same range.

4.2 Noise Characteristics

The noise power at the receiver can be expressed in terms of the system noise temperature ($T_{sys.}$) which is the sum of the antenna temperature ($T_{ant.}$) and the temperature of the devices between the antenna and the following receiver [11].

The noises from the environment include cosmic background noise, galactic noise, solar noise, earth noise, rain noise, and so on [12]. Among them, the rain noise is the major noise source in the Ka-band.

Assuming that the major lobe of an antenna points at a rain cloud with an ambient temperature of T_{rain}, then the antenna temperature can be expressed as a weighted sum of T_{rain} and T_{other} due to other noise sources as

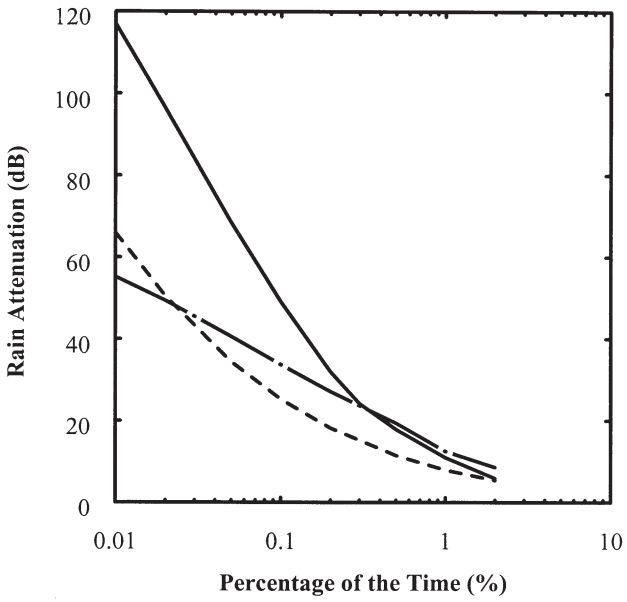

Fig. 6. Rain attenuation predicted by three rain models, latitude of ground station is 23°, elevation angle is 30°,——— : Crane model, - - - - - - : ITU-R model,——·—— :DAH model, f = 28.25 GHz.

$$T_{ant.} = w\, T_{rain} + (1 - w)\, T_{other} \tag{3}$$

where the weighting factor w is determined by the antenna radiation pattern.

For a rain cell or a rain cloud, the noise temperature (in °K) and the ambient temperature (T_m in °K) are related to each other by the rain attenuation (L_{rain} in dB) as [12]

$$T_{rain} = T_m\left(1 - 10^{-L_{rain}/10}\right) \tag{4}$$

The gaseous absorption accompanying rainfall is usually included in the rain attenuation.

4.3 Link Budget Calculation

The carrier-to-noise ratio of the complete link (from the ground station to the satellite, then back to the ground station) determines the quality of communication, and is combined from the carrier-to-noise-ratios of both the uplink and the downlink as [12], if we only consider the thermal noise

$$\left(\frac{C_t}{N_t}\right)^{-1} = \left(\frac{C_u}{N_u}\right)^{-1} + \left(\frac{C_d}{N_d}\right)^{-1} \tag{5}$$

where the subscripts t, u, and d stand for complete link, uplink, and downlink, respectively.

Since the radiation patterns of the ground station antennae have a very narrow beamwidth, coupling from the sidelobes that may cause multipath fading can be neglected. However, the satellite antennae have a very broad beamwidth that covers a wide area. To compensate for the free space loss variation as the satellite passes by a ground station, the radiation pattern is required to have a secant-like profile with respect to the pointing direction of the antennae. However, due to antenna imperfections, ripples of radiation pattern can exist in any plane (E-plane, H-plane, and so on). In our simulations, the measured radiation patterns of the satellite antennae are stored, and interpolation is used to obtain the antenna gain for any specific direction.

Assuming that the receiving antenna is at a distance r from the transmitting antenna, then the carrier-to-noise ratio can be expressed as

$$C/N_0 = EIRP - L_t + G_r / T_{sys.} - 228.6 \quad \text{in } dB_{HZ} \tag{6}$$

where N_0 is noise power per bandwidth, EIRP is the effective isotropic radiated power of the transmitting antenna, $L_t = L_{fs} + L_{rain} + L_{other}$ is the sum of free space loss, rain loss, and other losses (polarization mismatch, impedance mismatch, and so on), and G_r is the receiving antenna gain.

4.4 Simulation Schemes and Results

A coordinate system is defined with the center of the earth as the origin, the spinning axis of the earth as the Z axis, and another two mutually perpendicular lines as the X and Y axes. Then, the unit normal vector at the ground station can be expressed as

$$\hat{N}_R = \hat{X}\cos\theta_e \cos\Omega_e t + \hat{Y}\cos\theta_e \sin\Omega_e t + \hat{Z}\sin\theta_e$$

with Ω_e the angular speed of the earth spinning and θ_e the latitude of the ground station. If the satellite orbit is h above the mean sea level, then the radius of the satellite orbit is $R_s=R_e+h$ with R_e the radius of the earth. The flight speed of the satellite can be obtained by balancing the centrifugal force and the gravitational force. With h = 650/600/550 km, the satellite moves at about 7.546/7.573/7.600 km per second and takes about 97.84/96.80/95.77 minutes to move one round along its orbit.

Let $\hat{N}$ be the unit normal vector of the satellite orbital plane, and $\hat{M}$ be the unit position vector of the point where the orbit intercepts the X Z plane. Then, we have

$$\begin{aligned} \hat{N} &= -\hat{X}\sin\alpha + \hat{Z}\cos\alpha \\ \hat{M} &= \hat{X}\cos\alpha + \hat{Z}\sin\alpha \end{aligned} \tag{7}$$

The third unit vector on the orbital plane turns out to be $\hat{L} = \hat{M} \times \hat{N} = -\hat{Y}$. Assume that the satellite moves at an angular speed of Ω_s radians per second, then the position of the satellite can be expressed explicitly as

$$\bar{r}_T = \hat{L}R_s \cos\Omega_s t + \hat{M}R_s \sin\Omega_s t \tag{8}$$

Both the positions of the ground station and the satellite are updated at every time step of the simulation program.

The status of the communication link can be checked according to the following criterion

$$\cos^{-1}\left[\hat{N}_R \cdot (\bar{r}_T - \bar{r}_R)\Big/\left|\bar{r}_T - \bar{r}_R\right|\right] = \begin{cases} > 90°, & \text{beyond the horizon} \\ 75° \sim 90°, & \text{line - of - sight link, nontrackable} \\ 70° \sim 75°, & \text{line - of - sight link, trackable} \\ < 70°, & \text{line - of - sight link, in communication} \end{cases} \quad (9)$$

The tracking antenna on the ground station starts to track the satellite when it shows up on the horizon (antenna elevation angle between 0° and 15°), and the communication link is secured when the elevation angle is higher than 20°.

The simulation results over a one year period show that the in-sight time ranges widely from 75 to 475 seconds. About 46% of the links have an in-sight time of over 400 seconds. Some passes may have elevation angles lower than 20° throughout the pass, hence no communication link can be established. It is observed that 50% of the passes have their maximum elevation angle at between 15° to 40°.

The distribution of link time over one year period is shown in Figure 7. It is found that the link time may vary abruptly between two consecutive passes, and a greater maximum elevation angle implies a longer link time.

The simulation procedure is shown in Figure 8, in which a bit stream is transmitted from the ground station to the satellite, amplified by the transponder, then sent back to the ground

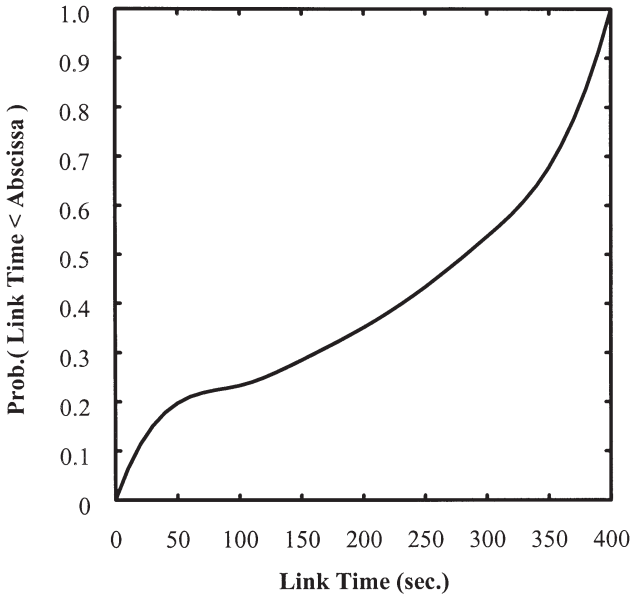

Fig. 7. Distribution of link time simulated over a one year period (2011 passes); orbit inclination angle is 35°, latitude of ground station is 23°N, and altitude of satellite is 600 km.

station.

The E_b/N_0 is related to C/N_0 as $C/N_0(dB_{HZ}) = E_b/N_0(dB) + R(dB_{HZ})$ where E_b is the bit energy and R is the transmission data rate. Either BPSK or QPSK is used in our simulation, and the bit-error-rate is10^{-3} (10^{-5}) when E_b/N_0= 6.7dB (9.7dB). With E_b/N_0= 6.7 dB and the bit rate of 6.6 Mbps, the associated C/N_0 is 74.9 dB_{HZ}.

Consider a specific pass in which the altitude of the satellite is 600 km and the orbit inclination angle is 35°. The in-sight time of this pass is 474 seconds, the link time is 396 seconds, and the maximum elevation angle is 86°.

The uplink rain loss over this pass at a rain rate of 5 mm / hr. is shown in Figure 9. The rain loss curves predicted by both the ITU-R and the DAH models look similar except that the

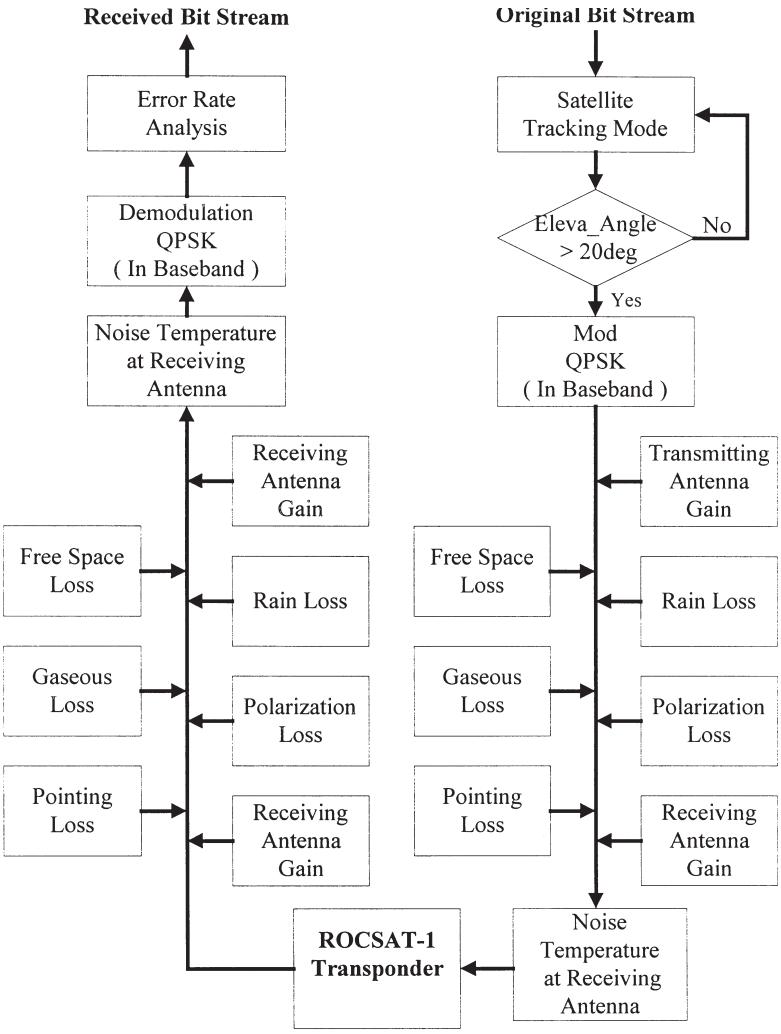

Fig. 8. Procedure of channel simulation on a bit stream.

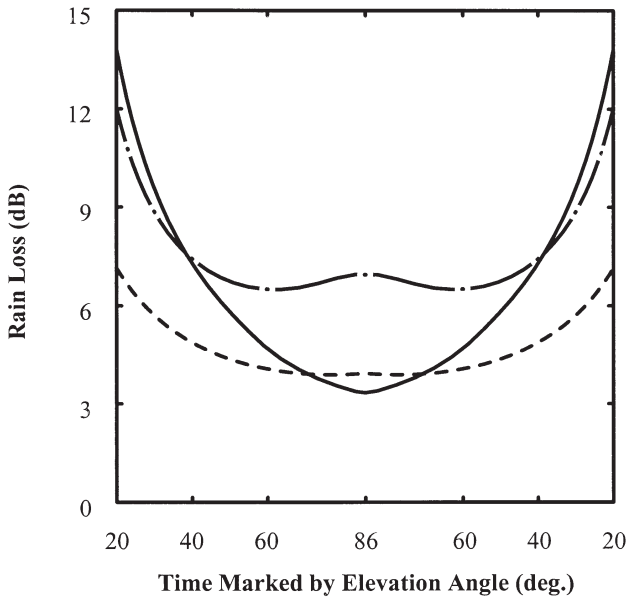

Fig. 9. Variation of rain attenuation at the rain rate of 5 mm/hr.,f=28.25 GHz, orbit inclination angle is 35°, latitude of ground station is 23°N, altitude of satellite is 600 km, in-sight time is 474 seconds, and link time is 396 seconds, ——— : Crane model, - - - - - : ITU-R model, —·— : DAH model.

DAH curve is about 3 dB higher than the ITU-R curve. The prediction by the ITU-R model has the least variation over all elevation angles, and the predictions by both the DAH and the Crane models become closer at low elevation angles. The rain loss curves predicted by the three models at the downlink have a shape similar to those in Figure 9, except that both the magnitude and the differences among three curves are reduced to about 40%.

The gaseous loss accompanying the rainfall is relatively negligible. The simulation shows that the gaseous loss at an elevation angle of 20° is 0.3 dB at the rain rate of 2 mm / hr., and is 0.64 dB at the rain rate of 53 mm / hr..

Figure 10 shows the antenna gain pointing toward the ground station as the satellite flies along this pass. Ripples are observed due to antenna imperfections as mentioned in the last subsection.

In rainy weather, the C/N_0 can be degraded to below the threshold, especially at low elevation angles. Figure 11 shows the predictions by using the three rain models. To keep the corresponding E_b/N_0 above the threshold, one can either reduce the transmission data rate or use only the portion of the link with greater elevation angles.

5. CONCLUSIONS

In preparation for the direct broadcast experiment of digital TV signals using Ka-band on

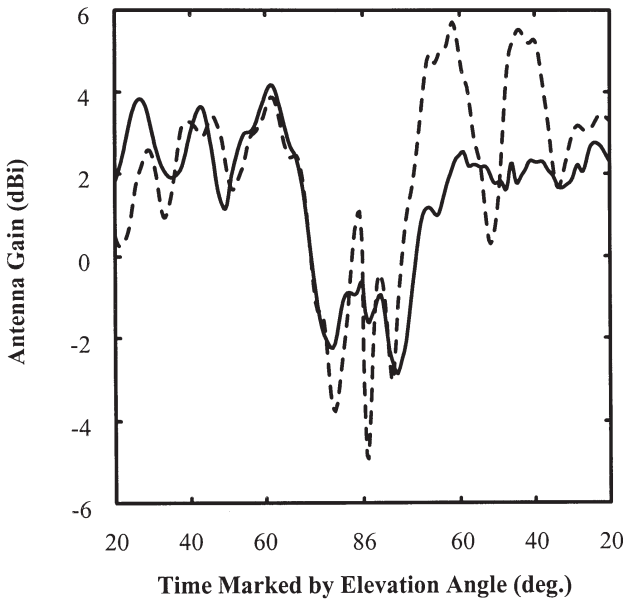

Fig. 10. Variation of satellite antenna gain pointing toward the ground station, the pass is the same as in *Fig. 9*, ——:transmitting antenna, - - - - - :receiving antenna.

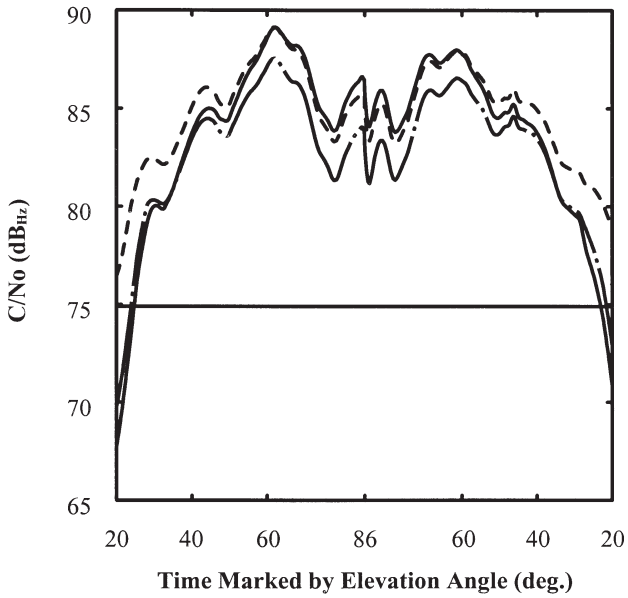

Fig. 11. Variation of C/N_0 at different rain rate, transmission data rate is 6.6 Mbps, rain rate is 5 mm/hr., the pass is the same as in *Fig. 9*, ——: Crane model, - - - - - :ITU-R model, —·— :DAH model.

ROCSAT-1, we have designed video and audio codecs, proposed error protection schemes and studied the characteristics of the communication link between the ground station and the satellite. Above all, a simulation program for the Ka-band channel has been developed, in which the effects of orbital parameters, power level, antenna data rate, and internal noise source on the carrier-to-noise ratio are taken into account. The simulation program aids the design of effective packet protection schemes and assessments of the communication performance of the ROCSAT-1 before its launch. After launch, the experiment will be continued for at least two years, and a realistic Ka-band channel model suitable for the subtropic Taiwan area will be developed.

Acknowledgements This research has been supported by the National Space Program Office (NSPO) of the Executive Yuan of the Republic of China. The author benefited much from discussions with Dr. Jo-Ku Hu, Dr. Ging-Shing Liu and many others from NSPO.

REFERENCES

[1] D. C. Hogg and T. S. Chu, September 1975: The role of rain in satellite communications. *Proc. IEEE*, **63**, 1308-1331.

[2] ISO/IEC DIS 13818-2, Information technology-generic coding of moving pictures and associated audio information - Part 2 : Video, November 1994.

[3] J.-F. Kiang, Y. C. Chen and L. G. Shi: Ka-band channel simulation on the LEO satellite, submitted to IEEE Trans. Antennas Propagat.

[4] Y. F. Hsu, Y. C. Chen, C. J. Huang and M. J. Sun, June 1998: MPEG-2 spatial scalable coding and transport stream error concealment for satellite TV broadcasting using Ka-band. *IEEE Trans. Broadcasting*, **44**, 233-242.

[5] Y. F. Hsu, C.H. Hsieh and Y. C. Chen : Embedded SNR scalable MPEG-2 video encoder and its associated error resilience decoding procedures, accepted by Signal Processing: Image Communication.

[6] Y. C. Chen, et al., June 1998: Scalable video codec design for direct broadcasting using Ka-band, yearly Technical Report to NSPO, NSC of the Repulibic of China, Taiwan.

[7] Advanced Television Systems Committee, Digital audio compression (AC-3) standard, Doc. A/52, December 1995.

[8] R. K. Crane, September 1980: Prediction of attenuation by rain. *IEEE Trans. Commun.* . **28**, 1717-1733.

[9] ITU Recommendation 838, ITU, Geneva, 1992.

[10] A. Dissanayake, J. Allnutt and F. Haidara, October, 1997: A prediction model that combines rain attenuation and other propagation impairment along earth-satellite paths. *IEEE Trans. Antennas Propagat,* **45**, 1564-1558.

[11] T. T. Ha, 1990: Digital Satellite Communications, New York: McGraw-Hill.

[12] G. D. Gordon and W. L. Morgan, 1993: Principles of Communication Satellites, New York: John Wiley.